TECHNICAL PAPER

New and efficient design of multimode piezoelectric vibration energy harvester for MEMS application

Osor Pertin[1] · Pinki Shrivas[1] · Koushik Guha[1] · K. Srinivasa Rao[2] · Jacopo Iannacci[3] ⓘ

Abstract

The major challenges in a piezoelectric energy harvester (PEH) are high operating frequency, narrow bandwidth and low output generation. We propose a new and efficient design concept based on optimal geometry shape and optimal segmentation of piezoelectric layer at strain nodes of higher vibration modes. The analytical model of the proposed design concept is developed and comparative analysis is performed to compare with conventional rectangular PEH and non-segmented trapezoidal PEH. For a mode 3 harvester design, the simulation result shows that there are three resonant peaks for voltage generation, at the fundamental, 2nd and 3rd resonant frequencies to enable multi-frequency operation that widens the operating frequency range of PEH. The parallel connection of the piezoelectric PZT segments to a common load resistance yields 21.6 mW, 0.23 mW and 0.15 mW power output for three resonant frequencies at 0.5 g input acceleration for optimal load of 21 kΩ. The proposed device shows a performance improvement and reduction in operating resonating frequencies of the higher modes of vibration compared to conventional rectangular and a non-segmented trapezoidal shaped PEH. The harvester provides an alternative to complex and inefficient device design of multimodal energy harvesters.

1 Introduction

Advances in low power Very Large Scale Integration (VLSI) design, CMOS Complementary Metal Oxide Semiconductor (CMOS) fabrication and MEMS Micro-Electro-Mechanical Systems (MEMS) technology have considerably reduced power requirements of devices. Energy harvesting is the process by which ambient energy is captured and converted into electricity for enabling self-powered devices. In the coming years, energy harvesting can totally eliminated the need for the battery as an energy source (Priya and Inman 2009). Recently, MEMS technology has been extensively used to realise micro energy

harvesters to meet the low power requirement of microelectronics and wireless sensors used in Internet of Things (IoT) application (Iannacci 2019). Replacing batteries in a wide wireless sensor network (WSN) can be tricky and expensive. Vibration Energy Harvester (VEH) has become increasingly popular as a self-sufficient and sustainable power solution for microsystem like WSN that is battery free (Roundy et al. 2004). A VEH uses ambient vibration to produce electrical energy using piezoelectric, electromagnetic and electrostatic transduction mechanisms (Priya and Inman 2009). Due to higher power density, ease of miniaturization, easy manufacturing and implementation, Piezoelectric Energy harvester (PEH) has been the focus of most researchers (Liu et al. 2018). PEHs are usually designed as unimorph or a bimorph cantilever beam and tip mass to reduce resonant frequency. They employ rectangular cantilever beams with a substrate and piezoelectric layer/layers where piezoelectric elements experience non-uniform strain that varies linearly along the length with maximum strain at the fixed end of cantilever beam (Yang et al. 2018). Overstrain and fatigue around the fixed end become concerns that can affect the lifetime of the PEH and have led the researchers to look for different geometries with more uniform strain distribution (Baker et al.

✉ Jacopo Iannacci
    iannacci@fbk.eu

1   Department of Electronics and Communication Engineering, National Institute of Technology, Silchar 788010, India

2   Electronics and Communication Engineering Department, KL University, Green Fields, Vaddeswaram, Guntur, Andhra Pradesh 522502, India

3   Center for Materials and Microsystems, Fondazione Bruno Kessler (FBK), Via Sommarive, 18, 38123 Trento, Italy

2005; Muthalif and Nordin 2015). To this end, tapered cantilevers with a trapezoidal profile are an optimal shape to improve power output for low frequency operation (Zhang et al. 2017). However flexible cantilever beams still suffer from disadvantage of high resonance frequency, narrow bandwidth and low voltage and power output. Additionally, ambient vibration source is typically random, low and wideband (Jones et al. 2001) and therefore a mechanism is required to lower the operating frequency and widen the operational bandwidth. Indrajit and Biswas (2018) showed that a device must be long, narrow and thin to have low resonant frequency (Indrajit and Biswas 2018). The classical vibration theory states that "higher vibration modes will have strain nodes, where the cancellation of charge occurs due to dynamic strain field changing direction along cantilever length (Erturk and Inman 2008)". The segmentation of electrode makes the piezoelectric harvester suitable for multi-mode frequency excitation (Erturk et al. 2009; Zizys et al. 2015). Alternatively, in order to resolve narrow bandwidth, multi DOF systems with multiple vibration modes have been used (Tang and Yang 2012; Nabavi 2019). The approach involves array of harvesters to realize multiple resonant structures thereby increasing the effective operational bandwidth. The major drawbacks of the method involves inefficient device volume since only a single harvester contributes to the device output at a particular frequency. Iannacci et al. (2015) proposed and experimentally verified a MEMS based VEH with Four-leaf Clover (FLC) design to achieve multimodality for wide operating frequency (Iannacci et al. 2015, 2016). The design concept exploits the same idea of increasing mechanical DOFs that enable multiple resonant modes of vibration for a single mechanical resonator structure. Furthermore, the complex design of FLC is optimized for suitable selected modes in order to lie in a predefined frequency band to find a trade-off between geometrical complexity and performance (Sordo et al. 2016; Janusas et al. 2014) experimentally evaluated multimode electromagnetic PEH with two resonant modes by not covering the strain nodes of second vibration mode having lower resonant frequency to match the environmental vibrations (Janusas et al. 2014). A similar finding is reported by Krishnasamy and Lenka (2018) where segmentation of piezoelectric layer has lower resonant frequency and improved power compared to segmentation of electrodes in both first and third vibration modes (Krishnasamy and Lenka 2018). Nonlinearity in a system is of great importance while designing any type of VEH (Ramlan et al. 2009). One method to achieve non-linearity is by varying nonlinear stiffness or motion by coupling with magnet, popularly known as piezo-magneto-elastic harvester. Shahruz (2008) investigated a piezoelectric harvester with a magnetic proof mass on the tip of

piezoelectric beam and magnets in its vicinity. He reported that when the magnets have appropriate strengths and is placed appropriately, the vibration of the beam-mass system can be amplified; thus increasing the harvested energy. The major drawbacks seen in implementation of nonlinear piezo-magneto-elastic harvesters are difficulty in micro manipulation and weight control of bulk magnet. Apart from narrow bandwidth and low power generation, fatigue becomes a concern for long-term vibration energy scavengers. In a PEH, 1600 microstrain for PZT unimorph film and 500 microstrain for bimorph is considered a strain safe limit to avoid fracture (Roundy et al. 2005).

To overcome the drawbacks of conventional linear PEHs, we propose a novel concept combining trapezoidal shaped PEH with segmented piezoelectric bimorph layers at the strain nodes of higher vibration modes of the PEH. The trapezoidal shape of the harvester will have more uniform strain distribution, which in turn results in efficient use of device structure for piezoelectric voltage generation while reducing the resonant operating frequency. Whereas, segmentation of bimorph piezoelectric layers further reduce the frequency and increase the generated output voltage by evading the cancellation of charge that occurs at strain nodes of higher vibration modes. The analytical model of the proposed design concept is also developed. The comparative analysis is performed between conventional rectangular PEH, non-segmented trapezoidal PEH and the proposed segmented trapezoidal PEH.

2 Model development and simulation

Figure 1 shows a schematic of continuous trapezoidal PEH. It has proof mass attached on beam's free end to adjust resonant frequency. PZT-5H is chosen as piezoelectric material because of its high volume of piezoelectric
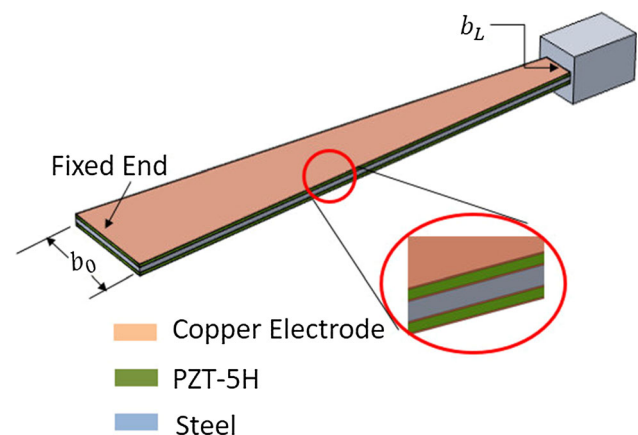
Fig. 1 Trapezoidal PEH with continuous bimorph piezoelectric PZT layers

coefficient and dielectric constant. Top and bottom of the steel substrate are attached with PZT layers. Thin electrodes are affixed on both side of PZT layers, which can be neglected for analytical models. The varying beam's width over the length L is given as,

$$b(x) = b_0 - cx, \ 0 \le x \le L \tag{1}$$

where, $c = (b_0 - b_L/L))$ is tapering parameter.

Equation of Motion (EoM) of a bimorph piezoelectric layer beam connected in parallel is given by Euler–Bernoulli assumptions (Erturk and Inman 2009),

$$\text{EI}(x)\frac{\partial^4 w(x,t)}{\partial x^4} + \vartheta(x)v(t)\left[\frac{d\delta(x)}{dx} - \frac{d\delta(x-L)}{dx}\right]$$
$$+ m(x)\frac{\partial^2 w(x,t)}{\partial t^2}$$
$$= -[M_t\delta(x-L) + m(x)]\frac{\partial^2 w_b(x,t)}{\partial t^2} \tag{2}$$

where, w_b is the excitation displacement of base in z direction, w is beam transverse deformation, $\delta(x)$ represents a Dirac delta function, $v(t)$ is the alternating piezoelectric voltage and M_t is mass of the tip. Rest of terms change along length as,

Bending stiffness,

$$\text{EI}(x) = b(x)\left[E_s\frac{h_s^3}{12} + \frac{2E_p}{3}\left(\left(\frac{h_s}{2} + h_p\right)^3 - \frac{h_s^3}{8}\right)\right] \tag{3}$$

Mass per unit length,

$$m(x) = b(x)(2\rho_p h_p + \rho_s h_s) \tag{4}$$

Electromechanical coupling term,

$$\vartheta(x) = b(x)\frac{E_p d_{31}}{h_p}\left[\left(\frac{h_s^3}{4}\right) - \left(h_p + \frac{h_s}{2}\right)^2\right] \tag{5}$$

where, the thickness of each PZT (h_p), thickness of Steel substrate (h_s), length of beam (L) are geometry parameters. ρ_p, ρ_s are density of PZT and steel respectively while E_p and E_s are the Young's modulus of PZT and steel material respectively. Table 1 shows the geometry and material properties of the structure.

Modal Analysis is important to find the mode shape of the vibrating beam. The transverse displacement of the beam is expressed using Galerkin procedure in the form (Erturk and Inman 2008),

$$w(x,t) = \sum_{i=1}^{n} \Phi_i(x)\eta_i(t) \tag{6}$$

where, $\Phi_i(x)$ is the mass normalized displacement eigenfunction and $\eta_i(x)$ is the coordinate of a cantilever beam of the ith mode. "The ith vibration mode has $i-1$ strain nodes (Erturk and Inman 2008)" and the ith mode shape

Table 1 Geometric dimension and material properties

Parameter	Description	Value
L	Length of beam	100 mm
b_0	Width of beam at fixed end (x = 0)	20 mm
b_L	Width of Beam at free end (x = L)	7 mm
h_p	Thickness of PZT	0.5 mm
h_s	Thickness of steel substrate	1 mm
d	Distance between two PZTs	0.2 mm
ρ_p	Density of PZT	7500 (kg/m^3)
ρ_s	Density of steel	7850 (kg/m^3)
E_p	Young's Modulus of PZT	64(GPa)
E_s	Young's Modulus of steel	200(GPa)
d_{31}	Piezoelectric constant	− 16.6(C/m^2)
ϵ_{ss}	Permittivity constant	25.55 (nF/m)
M_t	Tip Mass	11.8(mg)

$\Phi_i(x)$ is found by using above equations and the necessary boundary condition of a cantilever beam (fixed-free) as,

$$\Phi_i(x) = C_r\left[\cos\frac{\beta_r}{L}x - \cosh\frac{\beta_r}{L}x + \xi_r\left(\sin\frac{\beta_r}{L}x - \sinh\frac{\beta_r}{L}x\right)\right] \tag{7}$$

$$\xi_r = \frac{\sin\beta_r - \sinh\beta_r + \beta_r\frac{M_t}{m(x)L}(\cos\beta_r - \cosh\beta_r)}{\cos\beta_r + \cosh\beta_r + \beta_r\frac{M_t}{m(x)L}(\sin\beta_r - \sinh\beta_r)} \tag{8}$$

where, C_r is modal amplitude constant found by normalizing $\Phi_i(x)$ base on the orthogonality settings (Erturk and Inman 2009). And β_r is eigenvalues of the system obtained from characteristic equation

$$1 + \cos\beta\cosh\beta + \beta\frac{M_t}{m(x)L}(\cos\beta\sinh\beta - \sin\beta\cosh\beta) = 0 \tag{8}$$

Second derivative of the $\Phi_i(x)$ in Eq. (7) i.e. $\frac{d^2\Phi_i(x)}{dx^2}$ gives the strain distribution. For the trapezoidal bimorph beam shown in Fig. 1, the strain distribution curve is plotted for four modes (Fig. 2) in MATLAB. For a third mode of vibration, the strain nodes are found to be located at 0.1341 L and 0.4972 L as observed in Fig. 2, where L is the length of the beam.

Based on the strain distribution curve, the continuous trapezoidal beam of length L is segmented at 13.41 mm and 49.72 mm along the length to design segmented trapezoidal PEH for 3rd vibration mode. The final segmented trapezoidal model is shown in Fig. 3 that will work in 1st, 2nd and 3rd vibration modes.

Figure 4 shows the cross section of the bimorph cantilever beam with a substrate layer (h_s) sandwiched
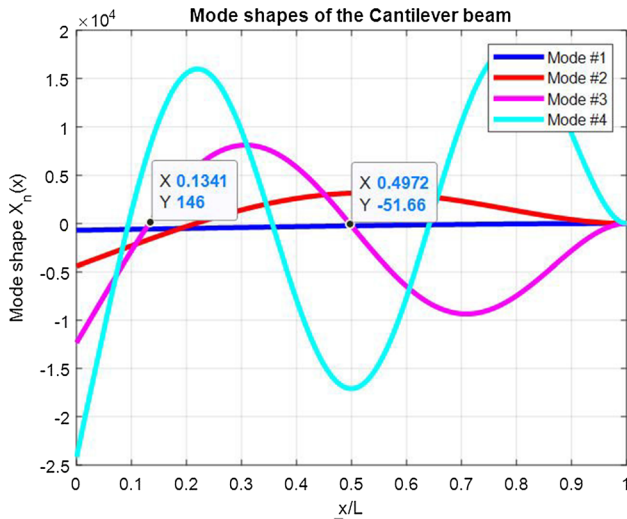
Fig. 2 Strain distribution curve of trapezoidal PEH for 1st, 2nd, 3rd and 4th vibration mode
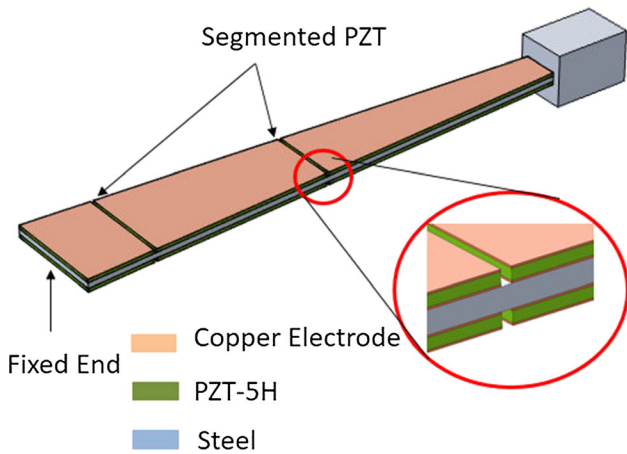

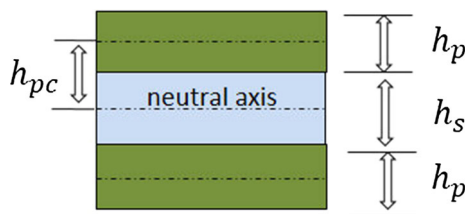Fig. 3 Proposed Segmented Trapezoidal PEH for 3rd mode of vibration

Fig. 4 Piezoelectric Beam cross section neglecting the thin electrode

between two piezoelectric layers (h_p). The discrete PZT layers created after segmentation are connected in parallel to a common load resistance R for maximum voltage as shown in Fig. 5.

The equivalent circuit is represented in Fig. 6. Where, $C_1 C_2$ and C_3 are equivalent capacitance of symmetric PZT
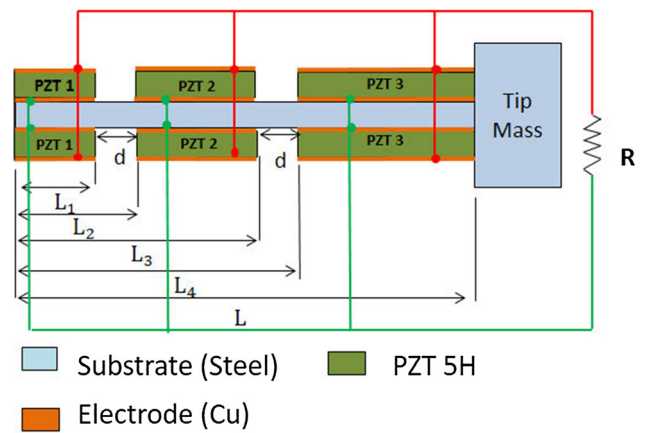

Fig. 5 Side view of beams with discrete piezoelectric segments of proposed PEH showing electrical connection
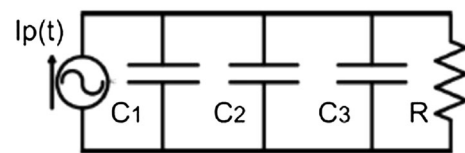

Fig. 6 Equivalent circuit of piezoelectric segments connected in parallel across a load resistance R

segments. The Kirchhoff's current equation gives the voltage-strain relationship (Krishnasamy and Lenka 2018),

$$\sum_{n=1}^{3} C_n(x) \frac{dv(t)}{dt} + \frac{v(t)}{R} - I_p(t) = 0 \tag{10}$$

$$C_1(x) = \frac{\varepsilon_{33} L_1 \int b(x)}{h_p}, 0 < x < L_1 \tag{11}$$

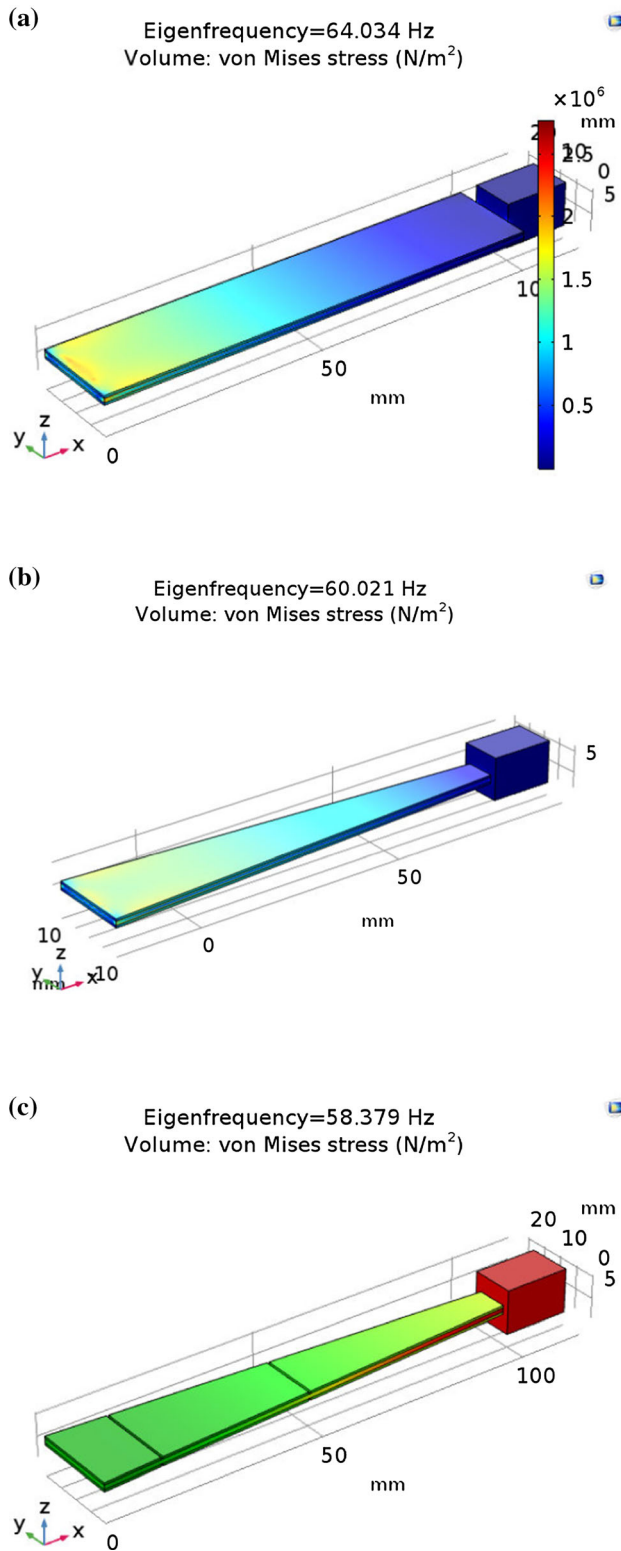$$C_2(x) = \frac{\varepsilon_{33}(L_3 - L_2) \int b(x)}{h_p}, L_2 < x < L_3 \tag{12}$$

$$C_3(x) = \frac{\varepsilon_{33}(L - L_4) \int b(x)}{h_p}, L_4 < x < L \tag{13}$$

$$I_p(t) = \sum_{n=1}^{3} \left(\int_{L_{i-1}}^{L_i} \left(b(x) E_p d_{31} h_{pc} \frac{\partial^3 w(x,t)}{\partial x^2 \partial t} + C_n(x) \frac{dv(t)}{dt} \right) dx \right) \tag{14}$$

$$h_{pc} = \frac{h_p + h_s}{2} \tag{15}$$

where i = 1, 3, 5 is segmented lengths of the beam. $L_5 = L$ is the total length and n is the number of PZT segments, n = 1($0 < x < L_1$), n = 2($L_2 < x < L_3$), n = 3 ($L_4 < x < L$) after segmentation. The constants d_{31} and ϵ_{33} gives the piezoelectric constant and permittivity of piezoelectric material respectively. The measured piezoelectric voltage is $v(t) = I_p(t) \times R$ across the load resistance. $P = \frac{v(t)^2}{R}$ gives the generated output power.

(a)

Eigenfrequency=64.034 Hz
Volume: von Mises stress (N/m²)

(b)

Eigenfrequency=60.021 Hz
Volume: von Mises stress (N/m²)

(c)

Eigenfrequency=58.379 Hz
Volume: von Mises stress (N/m²)

Fig. 7 FEM model of **a** rectangular PEH **b** trapezoidal PEH **c** segmented trapezoidal PEH in their fundamental mode of vibration with frequency 64 Hz, 60 Hz and 58.379 Hz respectively. The colour legend shows the von mises stress (N/m²) distribution
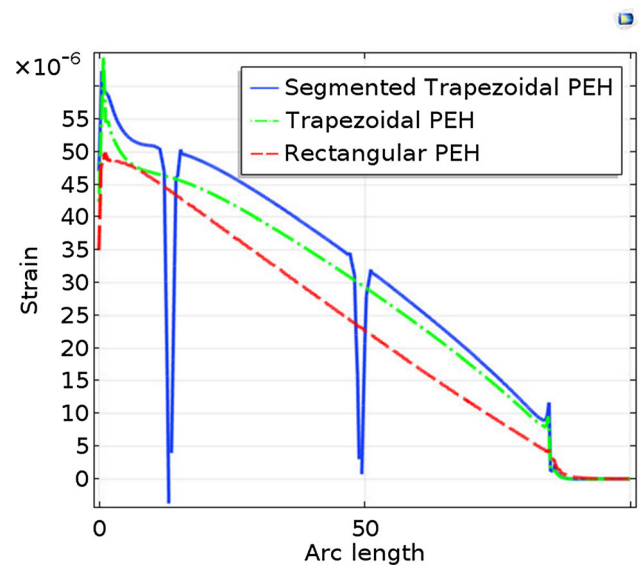
Fig. 8 Comparison of strain distribution of rectangular, trapezoidal, segmented trapezoidal piezoelectric energy harvester (PEH) along the length

The model is created using Finite Element Method (FEM) software COMSOL MULTIPHYSICS 5.5. The software calculates the generated piezoelectric output voltage and power generated using piezoelectric effect transduction in the piezoelectric harvester. The cantilever is constrained to be fixed at one end and the other end is free to vibrate. In terms of electrical boundary conditions, the inner faces of piezoelectric layer is grounded, while the top input acceleration of 0.5 g (g = 9.8 m/s^2) is applied to induce mechanical strain upon the device. The structure is meshed before performing any simulations analysis. The meshing has resulted in 26,256 elements for a total number of degrees of freedom of 169,463 for a segmented trapezoidal PEH. Eigen frequency study is done to find the Eigen frequencies and strain distribution of different vibration modes of the harvester. Frequency domain analysis is executed to study the performance across a frequency sweep around the resonant Eigen frequencies.

Figure 7 shows the FEM simulated model of the rectangular PEH (100 mm ×20mm), trapezoidal PEH and segmented PEH in their first mode of vibration having geometry and material properties as listed in table I. It can be seen from Fig. 7a that stress distribution of rectangular harvester is not uniform and is concentrated at fixed end of the cantilever beam. Figure 7b shows that stress distribution is improved a little in trapezoidal harvester compared to rectangular harvester while Fig. 7c shows stress distribution of segmented trapezoidal harvester is almost uniform along the entire length of the harvester.
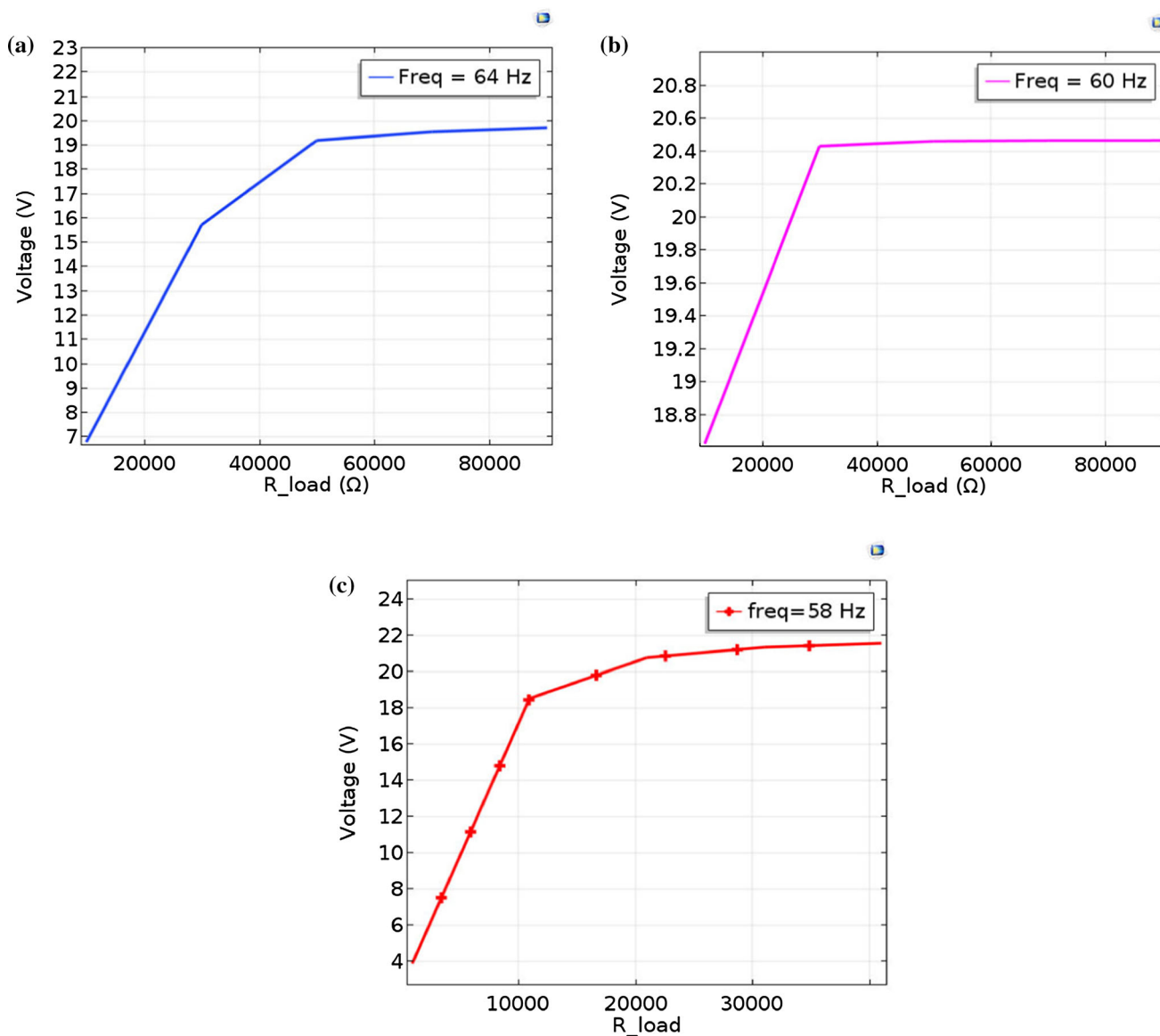
Fig. 9 Voltage vs. load resistance graph of **a** rectangular PEH **b** trapezoidal PEH **c** segmented trapezoidal PEH with 64 Hz, 60 Hz and 58 Hz respectively as input frequency in the fundamental mode (mode 1) of vibration
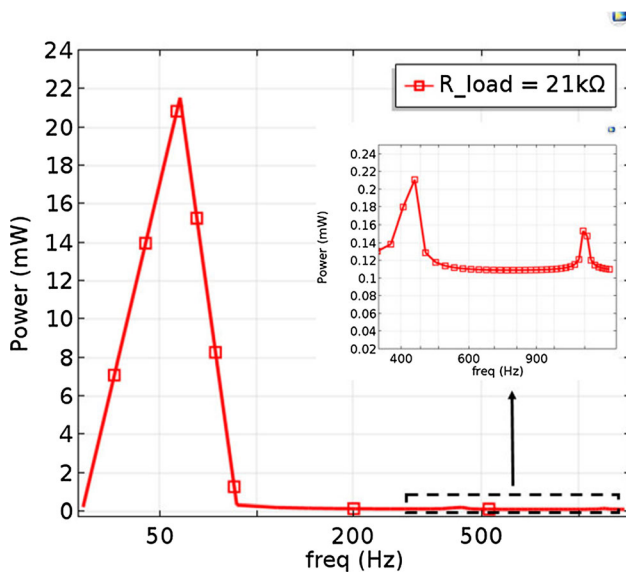
3 Result and discussion

In order to study the effect of introducing segmentation in an optimal trapezoidal shaped PEH, we used the FEM model with optimal geometry parameters to find the necessary output behaviour in the three vibration modes of the proposed harvester. The Fig. 8 compares the strain distribution of rectangular PEH, a trapezoidal PEH and the segmented trapezoid PEH in a graph. It can be observed that segmented trapezoid has more uniform strain along the length followed by continuous trapezoid and then rectangular harvester for same mechanical input. The undercut in strain distribution of segmented trapezoidal PEH as seen in Fig. 8 is due to discontinuity at strain nodes. The uniform

strain in trapezoidal shaped cantilever beam will reduce the fatigue concern due to concentration of strain around the fixed end of a rectangular cantilever beam.

The optimal electrical connection is found by finding the optimal load resistor connected across the output terminal as shown in Fig. 5. Figure 9a is the voltage vs. load resistance graph for a rectangular PEH that shows the voltage is maximum and gets saturated in 19.4 V for optimum load of 50 kΩ. Figure 9b shows that the optimal resistor of trapezoidal PEH is 26 kΩ at 20.4 V while the optimal load of segmented trapezoidal PEH is 21 kΩ at 21.3 V as shown in Fig. 9c. The reduced load resistor will increase the generated output power. Figure 10 shows the comparison of frequency response curve of rectangular
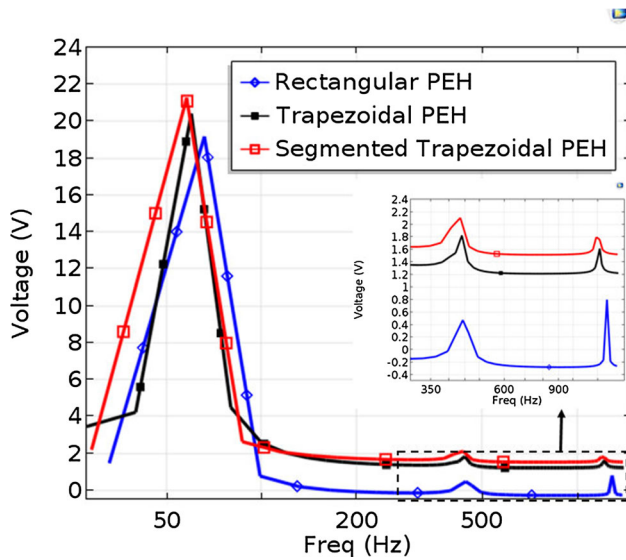
Fig. 10 Comparison of voltage generated at optimum load by rectangular PEH (50 kΩ), non-segmented trapezoidal PEH (26 kΩ) and segmented trapezoidal PEH (21 kΩ)

Fig. 11 Generated Output power of proposed segmented trapezoidal PEH for optimal load of 21 kΩ

Table 3 Comparison of Harvesters

Harvester Methodology	NPD (mWmm^{-2}g^{-2})
Segmented Bimorph PEH [10]	0.0023
Trapezoidal PEH [19]	0.023
Proposed PEH	0.064

PEH, trapezoidal PEH and segmented trapezoidal PEH for optimum load of 50 kΩ, 26 kΩ and 21 kΩ respectively at their respective resonant frequencies. The generated voltage is maximum at first fundamental resonant frequency in case of all the harvesters. The generated voltage is highest for segmented Trapezoidal PEH followed by trapezoidal PEH and rectangular PEH for all the three mode frequencies. There is resonance peak at three frequencies indicating multi frequency operation with increased power generation at higher vibration modes of the different harvesters. It is also observed that the operating resonant frequencies of the trapezoidal PEH is reduced compared to rectangular harvester, which is further reduced after segmentation of the piezoelectric PZT layers at strain nodes. Figure 11 shows the power generated in the proposed segmented trapezoidal PEH structure at optimum load of 21 kΩ. The generated power is 21.6 mW, 0.23 mW and 0.15 mW at three resonant frequencies 58 Hz, 400 Hz and 1189 Hz respectively. The generated outputs of the rectangular and trapezoidal piezoelectric energy harvester are tabulated in Table 2.

Table 2 summarises the output generated and makes a comparison of the rectangular PEH, trapezoidal PEH and segmented trapezoidal PEH in 1st, 2nd and 3rd vibration modes of the three harvester designs. There is increase in power generation by 91.66% at second vibration mode and improvement of 66.66% at third vibration mode after segmentation of bimorph piezoelectric PZT layers at strain nodes of trapezoidal PEH.

A comparative figure, area power density NPD (Normalize Power Density) with respect to both area and

Table 2 Summary and comparison of results

Parameter	Rectangular PEH			Trapezoidal PEH			Segmented Trapezoidal PEH		
	F_1	F_2	F_3	F_1	F_2	F_3	F_1	F_2	F_3
Frequency (Hz)	64	443	1283	60	430	1228	58	400	1189
Voltage (V)	19.2	0.47	0.8	20.4	1.8	1.6	21.3	2.2	1.8
Power (mW)	7.3	0	0.013	16	0.12	0.09	21.6	0.23	0.15

F_1, F_2, F_3 and are frequency at 1st, 2nd and 3rd vibration modes

acceleration is calculated as in (16) to compare the performance of the improved structure with previous work as tabulated in Table 3. The proposed harvester has improved NPD compared to previous optimized structures of PEH.

$$NPD = \frac{\text{Power}}{\text{Area} \times \text{acc}^2} \quad (16)$$

Before concluding this section, it is worth collecting some considerations around how the reported results could come to aid and support in other application fields of Microsystem (MEMS) technologies. In the first place, relying on a trapezoidal deformable beam to enhance the strain of the mass-spring system can improve the sensitivity of the miniaturised structure, if used for sensing purposes, e.g. inertial sensors or resonating sensor. Moreover, segmentation of electrodes might extend significantly the way mechanical deformations are transduced into electrical signals, therefore multiplying the sensing/actuating functions of the MEMS structure at stake. Finally, there exist aspects of reliability, as well, which are very important when dealing with Microsystem devices (Persano et al. 2016). To this end, the use of trapezoidal deformable structures can improve the mechanical reliability of MEMS-based devices.

4 Conclusion

The proposed PEH paves the way for a new and more practical design concept to improve the device performance with optimal geometry shape of the cantilever structure combined with segmentation concept. The trapezoidal shape offers a more uniform strain distribution to enable efficient use of the device volume while reducing the resonating frequency compared to conventional rectangular PEH. The segmentation of piezoelectric PZT layers at strain nodes of vibration mode avoids charge cancellation in the higher vibration modes thereby allowing it to operate in multi-mode with increased output generation. The harvester is designed for a 3rd by segmenting PZT at strain nodes, 13.41 mm and 49.72 mm along the length of the beam. Hence the proposed design has three operating resonant frequencies of 58 Hz, 400 Hz and 1200 Hz generating a power of 22.5 mW, 0.14 mW and 0.09 mW respectively at an optimum load resistance of 21 KΩ with 0.5 g input acceleration. Increase in power generation at 2nd vibration mode of 91.66% while an increase of 66.66% at third vibration mode is observed after segmentation of trapezoidal PEH. It is observed that segmentation of PZT layers further reduces the natural resonant frequency of the structure at higher vibration modes. It can be concluded that the proposed segmented trapezoidal design of

PEH reduces the operating resonant frequency with performance improvement at all three modes of vibration compared to conventional rectangular PEH and trapezoidal PEH. Since the device is within the safe strain limit with more uniform distributed strain along the length, the structure is more reliable and will have increased lifetime. A multi frequency harvester can be obtained from a single simple resonator structure and avoid design complexity. The design can be used as low frequency and wide band vibration energy harvester in low powering WSNs, wearable and implantable devices. Piezoelectric sensors are one of the fastest growing technology in sensor market. The obtained results of the study can also be exploited to optimize and improve the performance of piezoelectric micro sensors and micro actuators. The future effort should be to achieve close range frequencies of multimodal energy harvester.

References

Baker J, Roundy S, Wright P (2005) Alternative geometries for increasing power density in vibration energy scavenging for wireless sensor networks. In: 3rd International Energy Conversion Engineering Conference, San Francisco, California, https://doi.org/10.2514/6.2005-5617

Erturk A, Inman DJ (2008) A distributed parameter electromechanical model for cantilevered piezoelectric energy harvesters. ASME J Vib Acoust 130(4):041002-1-041002–15. https://doi.org/10.1115/1.2890402

Erturk A, Inman DJ (2009) An experimentallyvalidated bimorph cantilever model for piezoelectric energy harvesting frombase excitations. Smart Mater Struct 18(2):025009. https://doi.org/10.1088/0964-1726/18/2/025009

Erturk A, Tarazaga PA, Inman DJ (2009) Effect of strain nodes and electrode configuration on piezoelectric energy harvesting from cantilevered beams. J Vib Acoust 131(1):011010–011021. DOI:https://doi.org/10.1115/1.2981094

Iannacci J (2019) Microsystembased Energy Harvesting (EH-MEMS): powering pervasivity of the Internet ofThings (IoT)—a review with focus on mechanical vibrations. J King Saud Univ Sci 31:66–74. https://doi.org/10.1016/j.jksus.2017.05.019

Iannacci J, Sordo G, Serra E, Schmid U (2015) A novel MEMS-based piezoelectric multi-modal vibration energy harvester concept to power autonomous remote sensing nodes for Internet of Things (IoT) applications. In: IEEE SENSORS, Busan, pp 1–4. https://doi.org/10.1016/j.jksus.2017.05.019

Iannacci J, Sordo G, Serra E, Schmid U (2016) The MEMS four-leaf clover wideband vibration energy harvesting device: design concept and experimental verification. Springer Microsyst Technol 22:1865–1881. https://doi.org/10.1007/s00542-016-2886-3

Indrajit S, Biswas K (2018) Investigationof design parameters in mems based piezoelectric vibration energy harvester. 2018IEEE Electron Device Kolkata Conference (EDKCON), 24–25 November, 2018,Kolkata, India

Janusas G, Milasauskaite I, Ostasevicius V, Dauksevicius R (2014) Efficiency improvement of energy harvester at higher frequencies. J Vib Eng 16(3):1326–1333

Jones FG, Beeby SP, White NM (2001) Towards a piezoelectric vibration-powered microgenerator. IEE Proc Sci Mem Technol 148(2):68–72. https://doi.org/10.1049/ip-smt:20010323

Krishnasamy M, Lenka TR (2018) Distributed parameter modeling for autonomous charge extraction of various multilevel segmented piezoelectric energy harvesters. Microsyst Technol 24:1577–1587. https://doi.org/10.1007/s00542-017-3559-6

Liu H, Zhong J, Lee C, Lee SW, Lin L (2018) A comprehensive review on piezoelectric energy harvesting technology: materials, mechanisms, and applications. Appl Phys Rev 5:041306. https://doi.org/10.1063/1.5074184

Muthalif AGA, Nordin NHD (2015) Optimal piezoelectric beam shape for single and broadband vibration energy harvesting: modeling, simulation and experimental results. Mech Syst Signal Process 54–55:417–426. https://doi.org/10.1016/j.ymssp.2014.07.014

Nabavi S (2019) Nonlinear multi-modewideband piezoelectric MEMS vibration energy harvester. IEEE Sens J 19(13):4837–4848. https://doi.org/10.1109/JSEN.2019.2904025

Persano A, Quaranta F, Capoccia G, Proietti E, Lucibello A, Marcelli R, Bagolini A, Iannacci J, Taurino A, Siciliano P (2016) Influence of design and fabrication on RF performance of capacitive RF MEMS switches. Springer Microsyst Technol 22:1741–1746. https://doi.org/10.1007/s00542-016-2829-z

Priya S, Inman DJ (2009) Energy harvesting technologies. Springer Science Business Media, LLC, Berlin. https://doi.org/10.1007/978-0-387-76464-1 (ISBN: 978-0-387-76463-4)

Ramlan R, Brennan MJ, Mace BR, Kovacic I (2009) Potential benefits of a non-linear stiffness in an energy harvesting device. Nonlinear Dyn 59(4):545–558. DOI:https://doi.org/10.1007/s11071-009-9561-5

Roundy S, Wright PK, Rabaey JM (2004) Energy scavenging for wireless sensor networks:with special focus on vibrations. Kluwer Academic Publishers, Dordrecht (ISBN 978-1-4615-0485-6)

Roundy S, Leland E, Rivest J, Carleton E (2005) Improving power output for vibration-based energy Scavengers. Pervasive Comput IEEE 4:28–36. https://doi.org/10.1109/MPRV.2005.14

Shahruz SM (2008) Increasing the efficiency of energy scavengers by magnets. J Comput Nonlinear Dyn 3(4):041001. https://doi.org/10.1115/1.2960486. (12 pages)

Sordo G, Serra E, Schmid U, Iannacci J (2016) Optimization method for designing multimodal piezoelectric MEMS energy harvesters. Microsyst Technol 22(7):1811–1820. https://doi.org/10.1007/s00542-016-2848-9

Tang L, Yang Y (2012) A multiple-DOF piezoelectricenergy harvesting model. J Intell Mater Syst Struct 23(14):1631–1647. https://doi.org/10.1177/1045389X12449920

Yang Z, Zhou S, Zu J, Inman D (2018) High-performancepiezoelectric energy harvesters and their applications. Joule 2(4):642–697. https://doi.org/10.1016/j.joule.2018.03.011

Zhang G, Gao S, Liu H, Niu S (2017) A low frequency piezoelectric energy harvester with trapezoidal cantilever beam: theory and experiment. Microsyst Technol 23:3457–3466. https://doi.org/10.1007/s00542-016-3224-5

Zizys D, Rimvydas G, Rolanas D, Vytautas O, Vytautas D (2015) Segmentation of a vibrio-shock cantilever-type piezoelectric energy harvester operating in higher transverse vibration modes. Sensors 2016 16(1):11. doi:https://doi.org/10.3390/s16010011